

Simultaneously Altering the Energy Release and Promoting the Adhesive Force of an Electrophoretic Energetic Film with a Fluoropolymer

YanJun Yin,^{*,§} Yue Dong,[§] Mingling Li, and Zili Ma^{*}



Cite This: *Langmuir* 2022, 38, 2569–2575



Read Online

ACCESS |



Metrics & More

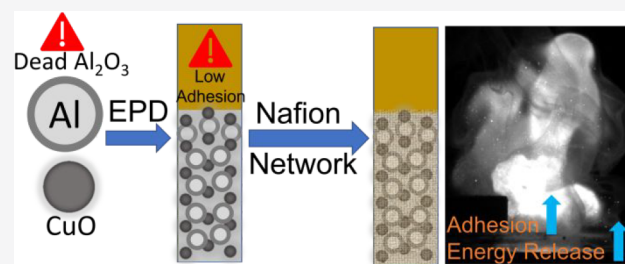


Article Recommendations



Supporting Information

ABSTRACT: Energetic coatings have attracted a great deal of interest with respect to their compatibility and high energy and power density. However, their preparation by effective and inexpensive methods remains a challenge. In this work, electrophoretic deposition was investigated for the deposition of an Al/CuO thermite coating as a typical facile effective and controllable method. Given the poor adhesion of the deposited film and the native inert Al_2O_3 shell on Al limiting energy output, further treatment was conducted by soaking in a Nafion solution, which not only acted as a fluoropolymer binder but also introduced a strong F oxidizer. It is interesting to note that the adhesion level of Al/CuO films was improved greatly from 1B to 4B, which was attributed to Nafion organic network film formation, like a fishing net covering the loose particles in the film. Combustion and energy release were analyzed using a high-speed camera and a differential scanning calorimeter. A combustion rate of ≤ 3.3 m/s and a heat release of 2429 J/g for Al/NFs/CuO are far superior to those of pristine Al/CuO (1.3 m/s and 841 J/g, respectively). The results show that the excellent combustion and heat release properties of the energetic film system are facilitated by the good combustion-supporting properties of organic molecules and the increase in the film density after organic treatment. The prepared Al/NFs/CuO film was also employed as ignition material to fire B- KNO_3 explosive successfully. This study provides a new way to prepare organic–inorganic hybrid energetic films, simultaneously altering the energy release and enhancing the adhesive force. In addition, the Al/NFs/CuO coating also showed considerable potential as an ignition material in microignitors.



INTRODUCTION

Thermite, a kind of composite energetic material (EM) consisting of solid metal fuel and oxidizer particles, have been applied in high-energy exchange components, such as electronic packaging, self-propagating welding, and self-propagating high-temperature diffusion welding.^{1,2} Reactive films as the typical form of thermite, also termed thermite laminates, have attracted a great deal of interest with respect to their compatibility and high energy and power density (superior to those of supercapacitors).³ Various applications of reactive coatings have been realized in microelectromechanical systems, microignitor devices, microelectronics, and bonding of materials.⁴

The properties of energetic films with large specific surface areas, low ignition delays, extremely high energy densities, and output efficiencies have been greatly improved due to the promotion of preparation technology, including magnetron sputtering, atomic deposition, spin coating, drop coating, etc.^{5,6} Compared with the coating method mentioned above, the film obtained by electrophoretic deposition (EPD) is more uniform and has fewer surface cracks with more excellent controllability.^{7,8} EPD, as an electrochemical method, is a process in which particles with charges in suspension are deposited onto

the substrate to form films through the action of a direct current electric field.^{9–12} EPD is used widely for electrophoretic paint and analysis and separation of natural colloid components, including proteins, polysaccharides, and nucleic acids.^{10,13}

After development for decades, EPD has become an important method for preparing thin film materials such as ceramics, metals, and oxide coatings. In recent years, EPD has been applied to the deposition of nanothermite films because of its simple process, short production cycle, controllable film thickness, shape, and high film quality.¹⁴ For instance, Al/ M_xO_y ($\text{M} = \text{Cu}, \text{Fe}, \text{Bi}, \text{Mo}, \text{Ni}, \text{Cr}$, etc.) thermite films can be obtained by EPD. The parameters related to the EPD process such as electrode type, electrode distance, dispersive medium, surfactant, voltage, and deposition time of the deposited film have been investigated in detail.¹⁵ The surface of the deposited

Received: November 26, 2021

Revised: January 16, 2022

Published: February 17, 2022



film can be kept flat, smooth, and even. However, the surface of the film is easy to fall off, chapped, and gapped and exhibits other poor adhesion phenomena after being affected by strong external forces, such as extrusion, friction, vibration, etc., which is one of the problems to be solved urgently in the current EPD process of the energetic films.⁹

Another problem for thermites is the native inert shell of Al_2O_3 and newly formed Al_2O_3 layers during the combustion process, which wrap the active Al fuel up and may hinder further reaction.^{16–18} In addition, the agglomeration of Al during the burning process can decrease the combustion efficiency.¹⁹ Therefore, managing the surface alumina layer to enhance the ignition and combustion of thermites is highly interesting. Researchers have demonstrated that fluorine can react with the dead Al_2O_3 layer forming a more volatile AlF_3 intermediate, which would facilitate the exposure of fresh Al for the further reaction.²⁰ Hence, adding additional fluorine-containing oxidizers to a system of thermites is a potential solution for increasing the energy density.

In addition to oxides, organic matter fluoropolymers also have been widely employed as oxidizers in Al-based energetic composites to enhance their energetic performance focusing as propellants, explosives, and pyrotechnics.^{16,21,22} Compared with inorganic oxides, fluoropolymers are more flexible to control. For example, three-dimensional (3D) printing technology can be used to construct a gradient structured polytetrafluoroethylene (PTFE)/Al composite coating.²³ A peak reaction heat of 7749.95 J/g was reached with a burning rate of ~ 130 mm/s. Although fluorine-containing materials can effectively improve the exothermic performance of energetic materials, the exploration of improving the adhesive force and combustion performance of granular energetic films is basically blank.²⁴

Among them, Nafion is one of the most typical fluoropolymers with a copolymer molecular architecture.²⁵ Its molecule is characterized by a hydrophobic polytetrafluoroethylene backbone chain [with the highest fluorine content (~ 76 wt %)] and regularly spaced shorter perfluorovinyl ether side chains terminated with a sulfonate ionic group.²⁶ Nafion has been used in various fields, such as a polymer electrolyte membrane, chloralkali electrolyzers, sensors, superacid catalysts, etc., because of its excellent thermal, mechanical, and chemical stability properties.^{27,28} Several commercial forms of Nafion are available, including member, fiber, and dispersions in aqueous alcohol solvents. As a film-forming resin, the dispersion form in solvents is extensively employed to prepare electrode films playing the role of an inorganic film-forming additive.²⁹ With regard to the application of Al combustion, it provides not only a strong fluorine oxidizer but also stable nanosized Al particles in ambient air.³⁰

Given the fluorine-rich and outstanding film-forming properties of Nafion, we were interested in tailoring the electrophoretic deposited inorganic thermite film by using Nafion. During the volatilization of the solvent, Nafion organic molecules can seep into the gap between particles and form a cross-linking net strengthening the connection between isolated particles and the substrate. Here, the energy release and adhesive force of hybrid energetic film were investigated.

EXPERIMENTAL SECTION

Reagents and Materials. Nano aluminum (50–100 nm, 99.9%, activity of 93.5%), $\text{Cu}(\text{NO}_3)_2 \cdot 6\text{H}_2\text{O}$, sucrose ($\text{C}_{12}\text{H}_{22}\text{O}_{11}$), H_2O_2 (30%), B (99%), KNO_3 (99%), isopropyl alcohol ($\text{C}_3\text{H}_8\text{O}$), and

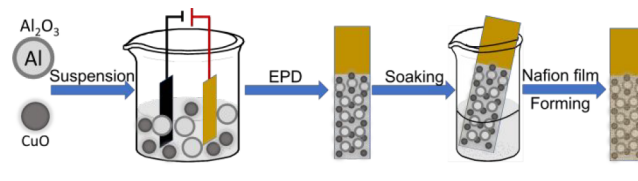
anhydrous ethanol ($\text{C}_2\text{H}_6\text{O}$) were commercially available from Shanghai Alighting Biochemical Technology Co., Ltd., without further purification. A Nafion 117 (NFs 117)-containing solution (~ 5 wt %) was provided by Sigma-Aldrich. A pure copper sheet (1 cm \times 2 cm, 99.99%) worked as the electrode in the EPD process. Deionized water was used throughout this study.

Fabrication of Porous Spherical CuO. For the preparation, CuO , $\text{Cu}(\text{NO}_3)_2 \cdot 6\text{H}_2\text{O}$ (1.938 g) and sucrose (0.3422 g) were added in 25 mL of H_2O by ultrasonication for 10 min, and 1 mL of H_2O_2 as the oxidant was added to this mixture while it was being strongly stirred. This solution was transferred to an autoclave, sealed, and heated at 180 °C for 12 h. After cooling to room temperature naturally, the product was centrifuged, washed with deionized water and anhydrous ethanol three to five times, and dried at 80 °C for 8 h in vacuum. Finally, the dried sample was annealed at 500 °C for 2 h to obtain pure CuO.

Electrophoretic Assembly of Al/CuO Thermite Films. Nano-Al and CuO were co-deposited on a copper sheet by EPD in a 50 mL suspension of isopropyl alcohol containing nano-Al (0.05 g) and CuO (0.1 g). The voltage for EPD was set at 150 V, and the deposition time was 10 min. Prior to EPD, the copper sheets were polished with sandpaper and ultrasonically cleaned for 10 min in ethanol, acetone, and deionized water. Two copper sheets with a 1 cm \times 2 cm exposed area were placed inside the organic suspension at a distance of 10 mm. The suspensions mentioned above for EPD were ultrasonicated for 10 min at room temperature. After EPD, Al/CuO coatings were dried for 3 h at 60 °C in a vacuum chamber.

Post-treatment of Al/CuO Thermite Coatings by NFs 117. To modify the deposited energetic films, the NFs 117 organics were first added to the Al/CuO system. Typically, the Al/CuO film was immersed in different concentrations (0, 0.2, 0.4, and 0.8 wt %) of a NFs 117 solution for 5 s, removed from the solution, and dried in vacuum at 60 °C for 12 h. The sample was labeled as Al/NFs/CuO. Scheme 1 shows the complete preparation procedure for the Al/NFs/CuO films.

Scheme 1. Schematic Illustration of the Preparation Procedure for the Al/NFs/CuO Films



Combustion Performance of Al/CuO and Al/NFs/CuO. A CO_2 continuous laser irradiation with a rated output power of 60 W and a laser spot diameter of <5.0 mm was employed to initiate the Al/CuO and Al/NFs/CuO coatings on a copper sheet in air. It should be noted that the length and width of the film to be measured should be consistent, and the ignition test should be uniformly started from the same end of the films. A standard optical ultra-high-speed industrial camera at an imaging speed of 6000 frames per second was used to characterize the combustion performance via capturing the flame and calculating the sustained combustion rate.

Boron and potassium nitrate (B-KNO_3), which were mixed at a 25:75 mass ratio, were used to characterize the initiation performance of Al/NFs/CuO and Al/CuO coatings.

Characterization. The surface morphology was observed by field emission scanning electron microscopy (FE-SEM, ZEISS Sigma 300) and Fourier transform infrared spectrophotometry (FT-IR, Nicolet IN10). X-ray diffraction (XRD) reflection patterns were recorded on a Rigaku D/Max 2500PC diffractometer with $\text{Cu K}\alpha$ radiation ($\lambda = 0.15405$ nm) at a scan rate of 5° min^{-1} . Additionally, differential scanning calorimetry (DSC, NETZSCH STA 449F3) was employed to characterize the heat release in the reaction performed from 30 to 1000 °C in free-standing ceramic crucibles with a heating rate of $10^\circ \text{ C min}^{-1}$ in a 99.999% argon atmosphere. Additionally, the ASTM

D3359-09 Standard Test Method for marking "X" Tape approved by the Department of Defense was used to evaluate the film adhesion.

RESULTS AND DISCUSSION

Structural Characterization. We first carried out XRD measurements to characterize the prepared CuO powder and Al/CuO and Al/NFs/CuO films. As shown in Figure 1a, the

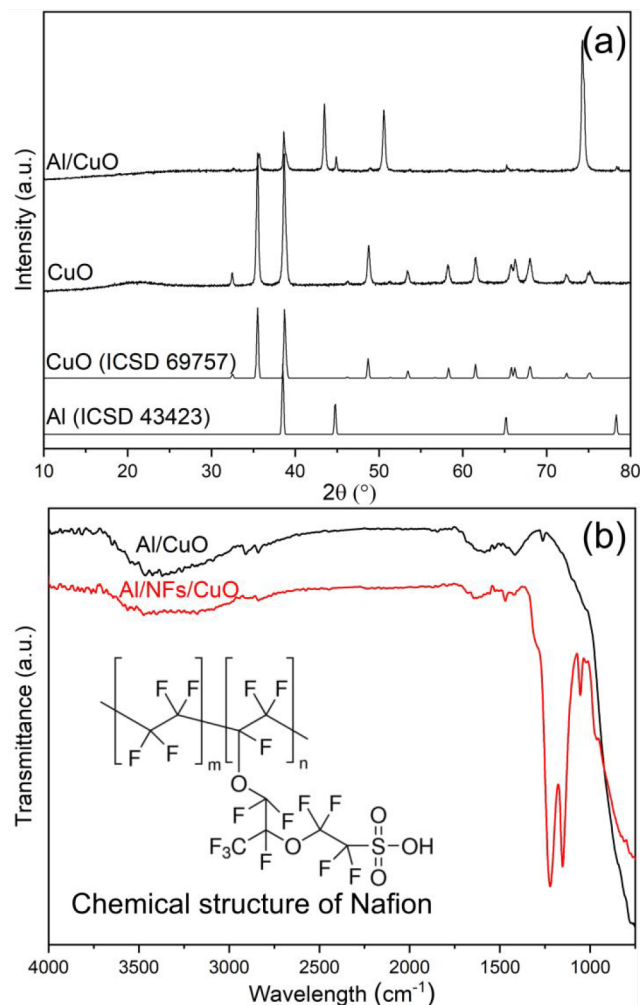


Figure 1. Characterization of the composition of samples: (a) XRD patterns of CuO and Al/CuO and (b) IR spectra of Al/CuO and Al/NFs/CuO.

experimental XRD pattern of CuO nicely matches with simulated XRD pattern of CuO (ICSD 69757), indicating the successful preparation of CuO. Furthermore, the representative diffraction peaks of CuO and Al were clearly detected in the as-deposited composite film according to the standard card of Al (ICSD 43423) and CuO (ICSD 69757). In addition, the peak positions of 43°, 51°, and 74° are assigned to the copper, which was from the copper substrate used to deposit Al/CuO films. The results demonstrated that the Al/CuO composite thermite coating was assembled efficiently via EPD. Because XRD was insufficient to detect any evidence for the presence of Nafion in the Al/NFs/CuO coating, complementary IR spectra were recorded to verify the presence of Nafion in the composite film. Figure 1b shows the IR spectra of Al/CuO and Al/NFs/CuO. Compared to the Al/CuO film, the Al/NFs/CuO film, which was post-treated

with a NFs solution, manifested more features in IR spectra. The peaks at 1153 and 1224 cm^{-1} were associated with a CF_2 symmetric stretching mode and an asymmetric stretching mode, respectively.³¹ The peaks at 1052 and 966 cm^{-1} correspond to the stretching vibration of the SO_3H group and COC group, respectively.³² The results indicate that NFs successfully filled the space between nano-Al and CuO particles forming a hybrid energetic film.

The as-prepared CuO powder via a hydrothermal method displays a porous microsphere shape (see Figure 2a). In the

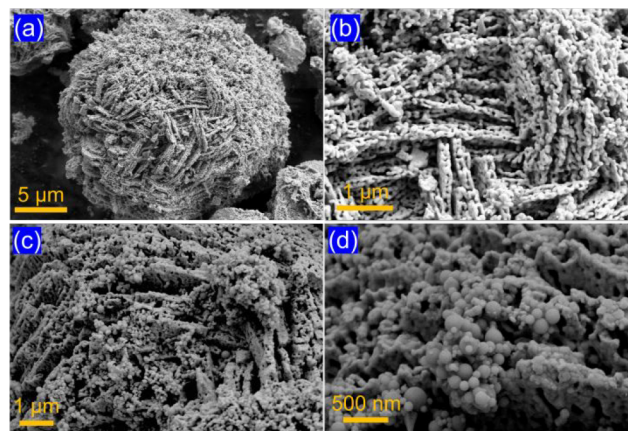


Figure 2. FE-SEM images of (a and b) CuO and (c and d) Al/CuO films.

enlarged view in Figure 2b, the surface of porous spherical CuO is rough and has an inherent porosity because of the burning of carbon during the calcination step.³³ After EPD, the Al/CuO composite coating was obtained on the copper sheet and characterized directly by FE-SEM. As depicted in Figure 2c, with pearl-like nano-Al spheres evenly inlaid on the surface of porous spherical CuO, the porous framework structure of CuO provides a nice platform for the uniform dispersion of nano-Al spheres. In a higher-magnification view in Figure 2d, the nano-Al spheres are embedded inside the skeleton of CuO compactly, which can increase the contact area between the nano-Al and CuO. The size and morphology of CuO and nano-Al do not change after EPD evidently, proving that EPD is a nondestructive process for the deposition of target particles.³⁴

It is generally known that NFs 117 is a kind of fluoropolymer with good film-forming ability. In the work presented here, a NFs 117 solution was used to post-treat Al/CuO thermite films with the goal of improving the adhesive force and energy release. The morphology of the Al/NFs/CuO energetic films impregnated with different concentrations of NFs 117 was found to change greatly compared with the pristine Al/CuO film, as shown in Figure 3. For the pristine Al/CuO film, the nano-Al and CuO particles are loosely piled together as judged from the low-magnification SEM image (Figure 3a). In the higher-magnification SEM image (inset of Figure 3a), the surface of the Al/CuO film is loose with cracks, showing a honeycomb structure. It is found that the content of the F element in the Al/CuO film gradually increases with an increase in the NFs solution concentration [see the SEM EDX mapping of the surface and cross section of the thermite film (Figures S1 and S2)]. The higher F content could accelerate the combustion of Al/CuO by exposing active Al, which is

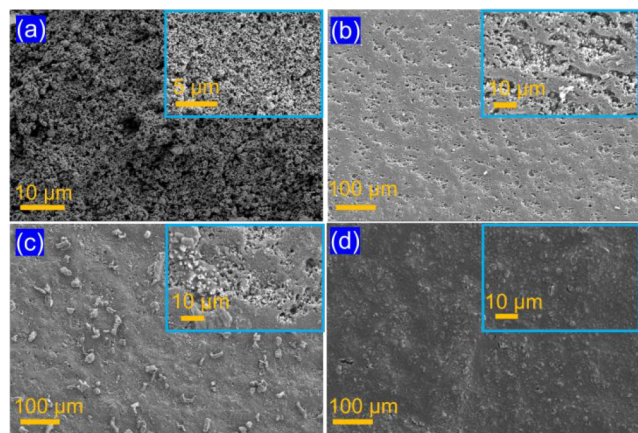


Figure 3. Typical FE-SEM images of the Al/CuO energetic films after treatment by NFs 117 at concentrations of (a) 0%, (b) 0.2%, (c) 0.4%, and (d) 0.8%.

consistent with the combustion test (Figure 5). During the EPD process, the film forms usually due to the electrostatic force between deposited particles and the substrate, and the adhesive force is generally weak.³⁵

It is interesting to note that the surface morphology of the Al/CuO film changed significantly after treatment even with a low concentration of NFs117 (see Figure 3b); most of the isolated particles are covered by the organic Nafion film. The thickness of the Al/CuO energetic film before and after treatment with NFs is $\sim 10\ \mu\text{m}$ (see the SEM images of the cross section of the films in Figure S2). Moreover, the NFs 117 solution can permeate the gap between the deep particles and contact the substrate and will cross-link after drying (see the SEM images of the cross section of the films in Figure S2). We can speculate that the cross-linked NFs films form a 3D-like network, which can anchor the particles in the network and enhance the adhesion. Upon observation at high magnification (inset of Figure 3b), the film surface was smooth but with many small holes because of the low concentration of NFs 117, leading to the defective coverage of the organic network film. We therefore increased the concentration of NFs solutions for impregnation. When the concentration of NFs 117 increased to 0.4%, the organic coverage of Al/CuO increased significantly and the small holes on the surface of the energetic films almost all disappeared, as shown in Figure 3c. Unsurprisingly, the density of the film was further enhanced when the concentration of NFs 117 reached 0.8% (see Figure 3d). One can clearly see that the nanoparticles were completely covered with the organic film or fused with the organic matter. No obvious cracks were observed.

Thermal Analysis and Combustion Performance. To quantitatively measure the energy density of the thermite films, the heat release of Al/CuO films before and after NFs treatment was compared in an argon atmosphere. The DSC curve shape of the four samples is similar consisting of two exothermic peaks, as shown in Figure 4. The heat output was obtained from the integral of the peak areas, which were 841, 2237, 2371, and 2429 J/g for the as-deposited Al/CuO film and after treatment with different concentrations of NFs. The results show that the heat release of the thermite films after treatment with NFs 117 (0.8%) increased by 1588 J/g (~ 2.9 times) compared with that of the pristine Al/CuO sample.

The four samples with the same mass (10 mg) were heated from room temperature to 1000 °C at a rate of 10 °C/min, and

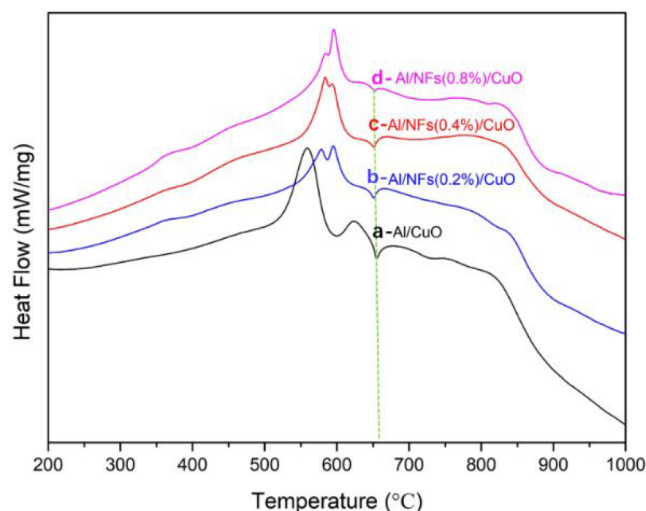


Figure 4. Heat release DSC plots of Al/NFs/CuO thermite films with NFs 117 concentrations of (a) 0%, (b) 0.2%, (c) 0.4%, and (d) 0.8%.

the melting point of Al nanoparticles did not change (660 °C) in the four systems. In addition, the reaction of the Al/CuO system began at 425 °C and ended at 900 °C. However, the initial reaction temperature for the Al/NFs (0.2%, 0.4%, 0.8%)/CuO films was $\sim 350\ ^\circ\text{C}$, which was lower than that of Al/CuO, and the end temperature was 900 °C. After treatment with a NFs solution, the initial reaction temperature of the Al/CuO system decreased, indicating the reaction was more sensitive. The sensitivity may benefit for the following two reasons. First, NFs, as an organic molecule, contains C, H, O, F, and other elements, which has certain flammability and can start the reaction at a lower temperature. Second, NFs has a low melting point (96 °C) and becomes a molten state during heating, which can bond nano-Al and CuO together well and conduct heat effectively, enabling Al and CuO to react quickly at a lower temperature. In addition, the Al/NFs (0.2%, 0.4%, 0.8%)/CuO DSC curves had only one exothermic peak, while two exothermic peaks were observed in the Al/CuO system. The main reason for the difference described above was the film-forming property of NFs, which wrapped the nano-Al and CuO into a denser composite, increasing their contact area and thus making their exothermic process more concentrated. There was only one exothermic peak in the range of 660–900 °C (i.e., after the melting of nano-Al) for the four systems. In conclusion, the Al/CuO energetic films treated with NFs show better exothermic performance, and the heat release of the system increases with an increase in NFs concentration. There are two main reasons for explaining the outstanding heat release performance phenomenon. First, NFs 117, as an organic compound, contains a variety of oxidizable elements such as F, O, etc., which has a good combustion-supporting property. Second, NFs 117 has good film-forming properties, forming an organic network on the surface of the Al/CuO film, binding loose particles, strengthening the density of the film, and improving the heat transfer efficiency effectively.^{36–38}

To test the combustion performance of the Al/CuO and Al/NFs/CuO micronano structure thermite film, a laser igniter was employed to trigger the sample and a high-speed camera was used to capture the flame for calculating the sustained combustion rate. After being irradiated with a laser, four samples responded quickly and produced a bright flame, accompanied by a self-propagating reaction with a violent

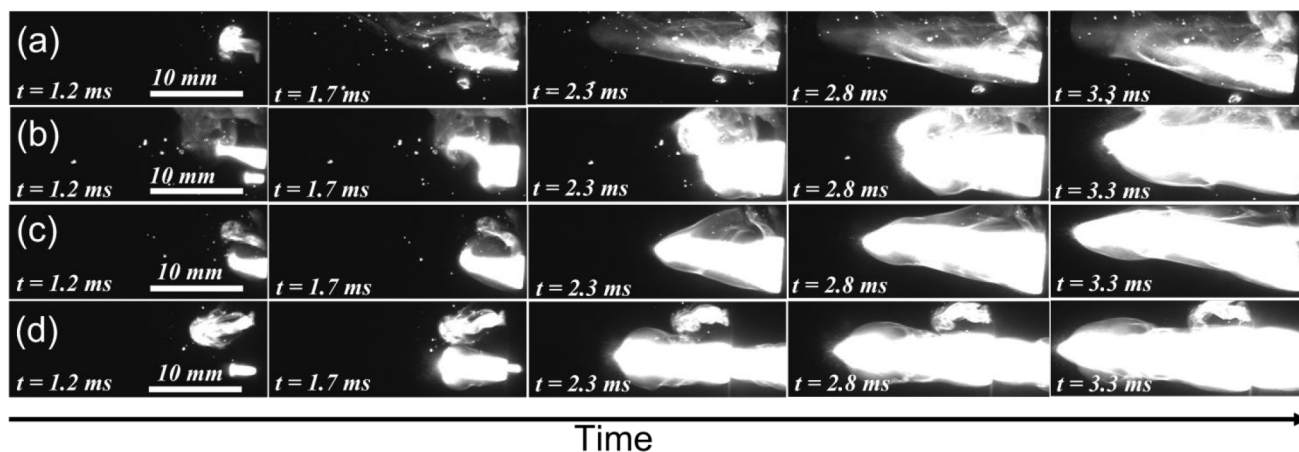


Figure 5. Combustion performance of Al/NFs/CuO thermite films with NFs 117 concentrations of (a) 0%, (b) 0.2%, (c) 0.4%, and (d) 0.8%.

exploding sound, as depicted in Figure 5. In terms of the overall effect, the burning intensity of the Al/NFs/CuO film was significantly promoted versus that of the pristine Al/CuO film, and the flame of the former sample was brighter with a more prominent flame length and width. The deep reason for the obvious difference in combustion performance was the effect of NFs on the redox process of the Al/CuO system. The combustion-supporting elements, especially F, in the organic NFs structure strengthen the combustion of Al and CuO. The burning intensity increased with an increase in NFs concentration. The highest flame can reach ~ 2.5 cm (see Figure 5d). Additionally, the combustion rates of the four samples are 1.3, 1.9, 2.7, and 3.3 m/s. These rates were consistent with the results of heat release.

Evaluation of Adhesion. Adhesion is an important aspect for evaluating the quality of micro/nano energetic material films. The ASTM D3359-09 standard test method approved by the U.S. Department of Defense was used to assess the adhesion of Al/CuO and Al/NFs/CuO coatings on the copper sheet. In the test process, a sharp and clean blade was operated to draw an "X" diagonally across the film. It should be noted that the "X" incision must penetrate the deposited film and reach the substrate. 3M tape was then stuck on the film surface seamlessly and tightly. Afterward, the tape was quickly peeled off from one end of the film to observe the exfoliation area of the powderous film for evaluating its adhesion level. There are generally six grades of adhesion from 0B to 5B. To ensure the authenticity, the tests described above were repeated three times. The results show that the adhesion grade was 1B for the Al/CuO film without NFs treatment, in which the surface of the film was exfoliated seriously with a peeling area of $>50\%$ (see Figure 6a). The adhesion of the energetic film was gradually improved after treatment with different concentrations of the NFs organic solvent. The posttreatment of the Al/CuO film with NFs 117 did not change the appearance of the films appreciably. Amazingly, the exfoliation area of the Al/NFs/CuO film was significantly decreased with an increase in the concentration of the NFs 117 solution (Figure 6). In other words, the adhesion of the Al/NFs/CuO film was enhanced remarkably. In Figure 6b, only a small block of film fell off close to the "X" part marked on the 3M tape. In panels c and d of Figure 6, the films were still intact except for only a tiny amount of shedding of powder accompanying the "X" mark. The adhesion levels of Figure 6b–d were determined as grades 2B–4B, respectively. The adhesion test results of the thermite

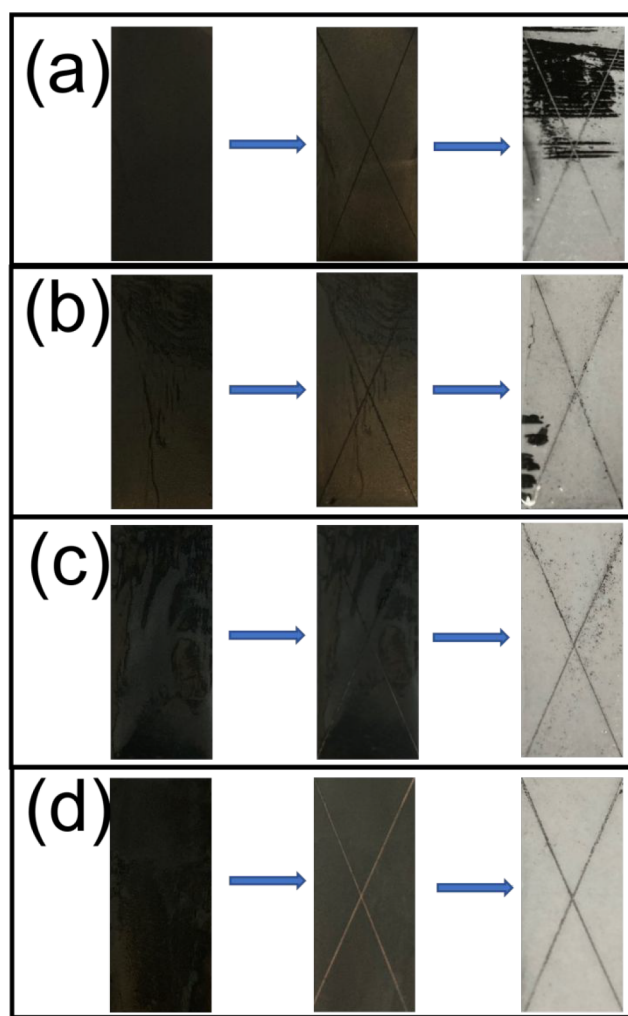


Figure 6. Al/NFs/CuO film adhesion test results with different additions of NFs 117: (a) 0%, (b) 0.2%, (c) 0.4%, and (d) 0.8%.

film are consistent with the results of SEM morphology analysis in Figure 3. The excellent film-forming ability of NFs solidifies the loose particle-based film, thus strengthening the adhesion of the film. When the particle-based film was post-treated with NFs, a 3D cross-linked NFs network would form and cross between particles and enhance the adhesion.

Firing of B-KNO₃. Boron-potassium nitrate (B-KNO₃) (25:75) is a well-known pyrotechnic composition, which is widely used in small-caliber rockets as well as pyrogen igniters for larger motors.³⁹ Nitramine explosives such as cyclo-trimethylenetrinitramine (RDX) and cyclotetramethylenetetranitramine (HMX) are widely used as ignition materials.⁴⁰ However, they are highly sensitive, limiting their use. In comparison with HMX and RDX, thermite-based energetic coatings are more insensitive. In Figure 7, the firing process of

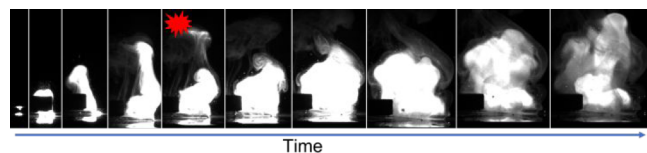


Figure 7. High-speed photographs of the ignition of B-KNO₃ via a thermite Al/NFs/CuO film.

B-KNO₃ by the Al/NFs/CuO film is presented. From the sequence of high-speed video frames, the Al/NFs/CuO film was first ignited via an electrical process and self-propagated quickly (see Movie S1). When the flame reached the B-KNO₃ explosive, a more violent and wider flame was observed (as marked in Figure 7; see Movie S1), indicating the B-KNO₃ explosive was fired successfully by the Al/NFs/CuO hybrid coating. To compare the ignition of B-KNO₃ by the thermite film, we have provided the ignition of B-KNO₃ via Al/CuO as well (see Figure S3, the ignition of B-KNO₃ via Al/CuO). The Al/CuO film with low adhesion also can ignite B-KNO₃, but with a low level of self-propagation. These results highlight the fact that the Al/NFs/CuO coating has considerable potential for use as an ignition material in microigniters.⁴¹

CONCLUSIONS

In this work, NFs 117 was first introduced into the energetic material system to enhance the adhesion of thermite coatings prepared by EPD. After the treatment of NFs117, the loose particles on the surface of the Al/CuO film are closely connected. The NFs film acts like a net covering the film surface, which strengthens the integrity of the Al/CuO film, making the adhesion of the thermite film increase from grade 1B to 4B. Moreover, the film combustion performance and heat release after treatment are promoted. In the Al/NFs (0.8%)/CuO film, the flame length is 2.5 cm, the burning rate reaches 3.3 m/s, and the heat release is 2429 J/g, which is much better than that of the pristine Al/CuO system. The excellent film-forming and combustion-supporting properties of the NFs 117 organic matter enhance the adhesion of the film, increase the effective contact area between particles, and improve the combustion effect. Organic substances, especially those containing fluorine, are expected to have outstanding performance in thermic film adhesion, combustion, and heat release and provide a research basis for the development and application of new energetic devices upon introduction into the field of energetic materials. In addition, the Al/NFs/CuO coating also shows considerable potential as an ignition material in microigniters.

ASSOCIATED CONTENT

Supporting Information

The Supporting Information is available free of charge at <https://pubs.acs.org/doi/10.1021/acs.langmuir.1c03170>.

SEM EDX image of the surface and cross section of thermite films and a comparison of the ignition process of B-KNO₃ via Al/CuO and Al/NFs/CuO (PDF)

Movie S1 (MP4)

AUTHOR INFORMATION

Corresponding Authors

YanJun Yin – Engineering Technology Center of Department of Education of Anhui Province, School of Chemistry and Material Engineering, Chaohu University, Chaohu 238024, China; orcid.org/0000-0002-9916-2784; Email: yanjunyin@chu.edu.cn

Zili Ma – Hefei National Laboratory for Physical Sciences at the Microscale, University of Science and Technology of China, Hefei 230026, China; orcid.org/0000-0001-7975-9201; Email: zлма@ustc.edu.cn

Authors

Yue Dong – Engineering Technology Center of Department of Education of Anhui Province, School of Chemistry and Material Engineering, Chaohu University, Chaohu 238024, China

Mingling Li – Engineering Technology Center of Department of Education of Anhui Province, School of Chemistry and Material Engineering, Chaohu University, Chaohu 238024, China

Complete contact information is available at: <https://pubs.acs.org/10.1021/acs.langmuir.1c03170>

Author Contributions

[§]Y.Y. and Y.D. contributed equally to this work.

Notes

The authors declare no competing financial interest.

ACKNOWLEDGMENTS

This work was supported by the National Natural Science Foundation of China (21905032), the Natural Science Foundation of the Higher Education Institutions of Anhui Province (KJ2019A0687), and the Innovation and Entrepreneurship Training Program for Students of Anhui Province (202010380014 and X202010380013). Y.Y. thanks Chaohu University for the Start-Up grant (KYQD-201907) and the Discipline Construction Quality Improvement Project (kj20zkjp01 and kj21kctd02). Z.M. thanks the Office of China Postdoc Council for the Talent Introduction Program of Postdoctoral International Exchange Program (YJ20210176). The authors thank the Shiyanjia lab (www.shiyanjia.com) for SEM and DSC measurements.

REFERENCES

- (1) Govender, D. R.; Focke, W. W.; Tichapondwa, S. M.; Cloete, W. E. Burn Rate of Calcium Sulfate Dihydrate–Aluminum Thermites. *ACS Appl. Mater. Interfaces* **2018**, *10* (24), 20679–20687.
- (2) Ma, X.; Li, Y.; Hussain, I.; Shen, R.; Yang, G.; Zhang, K. Core–Shell Structured Nanoenergetic Materials: Preparation and Fundamental Properties. *Adv. Mater.* **2020**, *32* (30), 2001291.
- (3) Rossi, C.; Zhang, K.; Esteve, D.; Alphonse, P.; Tailhades, P.; Vahlas, C. Nanoenergetic Materials for MEMS: A Review. *J. Microelectromechanical Syst.* **2007**, *16* (4), 919–931.
- (4) Wang, J.; Zhang, W.; Wang, L.; Shen, R.; Xu, X.; Ye, J.; Chao, Y. Novel Approach to the Preparation of Organic Energetic Film for Microelectromechanical Systems and Microactuator Applications. *ACS Appl. Mater. Interfaces* **2014**, *6* (14), 10992–10996.

- (5) Zapata, J.; Nicollet, A.; Julien, B.; Lahiner, G.; Esteve, A.; Rossi, C. Self-Propagating Combustion of Sputter-Deposited Al/CuO Nanolaminates. *Combust. Flame* **2019**, *205*, 389–396.
- (6) Muravyev, N. V.; Monogarov, K. A.; Schaller, U.; Fomenkov, I. V.; Pivkina, A. N. Progress in Additive Manufacturing of Energetic Materials: Creating the Reactive Microstructures with High Potential of Applications. *Propellants, Explos. Pyrotech.* **2019**, *44* (8), 941–969.
- (7) Chiang, Y.-C.; Wu, M.-H. Assembly and Reaction Characterization of a Novel Thermite Consisting Aluminum Nanoparticles and CuO Nanowires. *Proc. Combust. Inst.* **2017**, *36* (3), 4201–4208.
- (8) Sullivan, K. T.; Worsley, M. A.; Kuntz, J. D.; Gash, A. E. Electrophoretic Deposition of Binary Energetic Composites. *Combust. Flame* **2012**, *159* (6), 2210–2218.
- (9) Yin, Y.; Li, X. Electrophoretic Deposition and Characterization of an Al/CuO Energetic Film with a Porous Hollow Microsphere Structure. *J. Mater. Eng. Perform.* **2020**, *29* (2), 1375–1383.
- (10) Yin, Y.; Li, X. Al/CuO Composite Coatings with Nanorods Structure Assembled by Electrophoretic Deposition for Enhancing Energy Released. *Vacuum* **2019**, *163*, 216–223.
- (11) Ma, Z.; Jaworski, A.; George, J.; Rokicinska, A.; Thersleff, T.; Budnyak, T. M.; Hautier, G.; Pell, A. J.; Dronskowski, R.; Kuśtrowski, P.; Slabon, A. Exploring the Origins of Improved Photocurrent by Acidic Treatment for Quaternary Tantalum-Based Oxynitride Photoanodes on the Example of CaTaO_2N . *J. Phys. Chem. C* **2020**, *124* (1), 152–160.
- (12) Ma, Z.; Chen, K.; Jaworski, A.; Chen, J.; Rokicińska, A.; Kuśtrowski, P.; Dronskowski, R.; Slabon, A. Structural Properties of $\text{NdTiO}_{2-x}\text{N}_{1-x}$ and Its Application as Photoanode. *Inorg. Chem.* **2021**, *60* (2), 919–929.
- (13) Yin, Y.; Li, X.; Shu, Y.; Guo, X.; Zhu, Y.; Huang, X.; Bao, H.; Xu, K. Highly-Reactive Al/CuO Nanoenergetic Materials with a Tubular Structure. *Mater. Des.* **2017**, *117*, 104–110.
- (14) Zhang, D.; Xiang, Q. Electrophoretic Fabrication of an Al- Co_3O_4 Reactive Nanocomposite Coating and Its Application in a Microignitor. *Ind. Eng. Chem. Res.* **2016**, *55* (30), 8243–8247.
- (15) Zhang, D.; Pei, R.; Peng, X.; Xiang, Q.; Wang, X. Environment-Friendly Formation of High Energetic Nano-Al/ Fe_2O_3 Bilayer by Aqueous Electrophoretic Deposition. *Propellants, Explos. Pyrotech.* **2019**, *44* (12), 1600–1607.
- (16) Jiang, Y.; Deng, S.; Hong, S.; Tiwari, S.; Chen, H.; Nomura, K.; Kalia, R. K.; Nakano, A.; Vashishta, P.; Zachariah, M. R.; Zheng, X.; et al. Synergistically Chemical and Thermal Coupling between Graphene Oxide and Graphene Fluoride for Enhancing Aluminum Combustion. *ACS Appl. Mater. Interfaces* **2020**, *12* (6), 7451–7458.
- (17) Agarwal, P. P. K.; Jensen, D.; Chen, C.-H.; Rioux, R. M.; Matsoukas, T. Surface-Functionalized Boron Nanoparticles with Reduced Oxide Content by Nonthermal Plasma Processing for Nanoenergetic Applications. *ACS Appl. Mater. Interfaces* **2021**, *13* (5), 6844–6853.
- (18) Westphal, E. R.; Murray, A. K.; McConnell, M. P.; Fleck, T. J.; Chiu, G. T. C.; Rhoads, J. F.; Gunduz, I. E.; Son, S. F. The Effects of Confinement on the Fracturing Performance of Printed Nanothermites. *Propellants, Explos. Pyrotech.* **2019**, *44* (1), 47–54.
- (19) Zhu, B.; Zhang, S.; Sun, Y.; Ji, Y.; Wang, J. Fluorinated Graphene Improving Thermal Reaction and Combustion Characteristics of Nano-Aluminum Powder. *Thermochim. Acta* **2021**, *705* (June), 179038.
- (20) Kappagantula, K. S.; Farley, C.; Pantoya, M. L.; Horn, J. Tuning Energetic Material Reactivity Using Surface Functionalization of Aluminum Fuels. *J. Phys. Chem. C* **2012**, *116* (46), 24469–24475.
- (21) Li, X.; Guerieri, P.; Zhou, W.; Huang, C.; Zachariah, M. R. Direct Deposit Laminate Nanocomposites with Enhanced Propellant Properties. *ACS Appl. Mater. Interfaces* **2015**, *7* (17), 9103–9109.
- (22) Wang, H.; Kline, D. J.; Rehwooldt, M.; Wu, T.; Zhao, W.; Wang, X.; Zachariah, M. R. Architecture Can Significantly Alter the Energy Release Rate from Nanocomposite Energetics. *ACS Appl. Polym. Mater.* **2019**, *1* (5), 982–989.
- (23) Zheng, D.; Huang, T.; Xu, B.; Zhou, X.; Mao, Y.; Zhong, L.; Gao, B.; Wang, D. 3D Printing of N-Al/Polytetrafluoroethylene-Based Energy Composites with Excellent Combustion Stability. *Adv. Eng. Mater.* **2021**, *23* (5), 2001252.
- (24) Huang, S.; Hong, S.; Su, Y.; Jiang, Y.; Fukushima, S.; Gill, T. M.; Yilmaz, N. E. D.; Tiwari, S.; Nomura, K.; Kalia, R. K.; et al. Enhancing Combustion Performance of Nano-Al/PVDF Composites with β -PVDF. *Combust. Flame* **2020**, *219*, 467–477.
- (25) Haubold, H.-G.; Vad, T.; Jungbluth, H.; Hiller, P. Nano Structure of NAFION: A SAXS Study. *Electrochim. Acta* **2001**, *46* (10–11), 1559–1563.
- (26) Jansto, A.; Davis, E. M. Role of Surface Chemistry on Nanoparticle Dispersion and Vanadium Ion Crossover in Nafion Nanocomposite Membranes. *ACS Appl. Mater. Interfaces* **2018**, *10* (42), 36385–36397.
- (27) Hwang, M.; Karenson, M. O.; Elabd, Y. A. High Production Rate of High Purity, High Fidelity Nafion Nanofibers via Needleless Electrospinning. *ACS Appl. Polym. Mater.* **2019**, *1* (10), 2731–2740.
- (28) Yamato, T.; Hideshima, C.; Prakash, G. K. S.; Olah, G. A. Organic Reactions Catalyzed by Solid Supercacids. 5. Perfluorinated Sulfonic Acid Resin (Nafion-H) Catalyzed Intramolecular Friedel-Crafts Acylation. *J. Org. Chem.* **1991**, *56* (12), 3955–3957.
- (29) Ma, Z.; Guo, C.; Yin, Y.; Zhang, Y.; Wu, H.; Chen, C. The Use of Cheap Polyaniline and Melamine Co-Modified Carbon Nanotubes as Active and Stable Catalysts for Oxygen Reduction Reaction in Alkaline Medium. *Electrochim. Acta* **2015**, *160*, 357–362.
- (30) Li, H.; Mezziani, M. J.; Lu, F.; Bunker, C. E.; Gulians, E. A.; Sun, Y.-P. Templated Synthesis of Aluminum Nanoparticles - A New Route to Stable Energetic Materials. *J. Phys. Chem. C* **2009**, *113* (48), 20539–20542.
- (31) Liang, Z.; Chen, W.; Liu, J.; Wang, S.; Zhou, Z.; Li, W.; Sun, G.; Xin, Q. FT-IR Study of the Microstructure of Nafion® Membrane. *J. Membr. Sci.* **2004**, *233* (1–2), 39–44.
- (32) Yeager, H. L.; Steck, A. Cation and Water Diffusion in Nafion Ion Exchange Membranes: Influence of Polymer Structure. *J. Electrochem. Soc.* **1981**, *128* (9), 1880–1884.
- (33) Ma, Z.; Chen, J.; Luo, D.; Thersleff, T.; Dronskowski, R.; Slabon, A. Structural Evolution of CrN Nanocube Electrocatalysts during Nitrogen Reduction Reaction. *Nanoscale* **2020**, *12* (37), 19276–19283.
- (34) Yin, Y.; Li, X. Building Energetic Material from Novel Salix Leaf-like CuO and Nano-Al through Electrophoretic Deposition. *Bull. Korean Chem. Soc.* **2016**, *37* (11), 1827–1830.
- (35) Zhu, Y.; Li, X.; Zhang, D.; Bao, H.; Shu, Y.; Guo, X.; Yin, Y. Tuning the Surface Charges of MoO_3 by Adsorption of Polyethylenimine to Realize the Electrophoretic Deposition of High-Exothermic Al/ MoO_3 Nanoenergetic Films. *Mater. Des.* **2016**, *109*, 652–658.
- (36) DeLisio, J. B.; Hu, X.; Wu, T.; Egan, G. C.; Young, G.; Zachariah, M. R. Probing the Reaction Mechanism of Aluminum/Poly(vinylidene fluoride) Composites. *J. Phys. Chem. B* **2016**, *120* (24), 5534–5542.
- (37) Sippel, T. R.; Son, S. F.; Groven, L. J. Aluminum Agglomeration Reduction in a Composite Propellant Using Tailored Al/PTFE Particles. *Combust. Flame* **2014**, *161* (1), 311–321.
- (38) Ye, M.; Zhang, S.; Liu, S.; Han, A.; Chen, X. Preparation and Characterization of Pyrotechnics Binder-Coated Nano-Aluminum Composite Particles. *J. Energy Mater.* **2017**, *35* (3), 300–313.
- (39) Krishnan, K. R. R.; Ammal, R. A.; Hariharanath, B.; Rajendran, A. G.; Kartha, C. B. Addition of RDX/HMX on the Ignition Behaviour of Boron-Potassium Nitrate Pyrotechnic Charge. *Def. Sci. J.* **2006**, *56* (3), 329–338.
- (40) Yan, Q.-L.; Zhao, F.-Q.; Kuo, K. K.; Zhang, X.-H.; Zeman, S.; DeLuca, L. T. Catalytic Effects of Nano Additives on Decomposition and Combustion of RDX-, HMX-, and AP-Based Energetic Compositions. *Prog. Energy Combust. Sci.* **2016**, *57*, 75–136.
- (41) Ma, X.; Cheng, S.; Hu, Y.; Ye, Y.; Shen, R. Integrating Micro-Ignitors with Al/Bi 2O_3 /Graphene Oxide Composite Energetic Films to Realize Tunable Ignition Performance. *J. Appl. Phys.* **2018**, *123* (9), 095305.